AIAA JOURNAL
Vol. 44, No. 1, January 2006

Air Pressure Effect on Propulsion with Transversly Excited Atmospheric CO_2 Laser

Andrew V. Pakhomov* and Jun Lin†
University of Alabama in Huntsville, Huntsville, Alabama 35899
and
Rongqing Tan‡
Chinese Academy of Sciences, 100080 Beijing, People's Republic of China

The assessment of energy partition between air and solid propellant has been conducted using a transversely excited atmospheric CO_2 laser. The experiments were performed by focusing output pulses of the laser (200-ns pulsewidth at 10.6-μm wavelength and $\sim$10.6-J pulse energy) on aluminum targets mounted on a ballistic pendulum. Coupling coefficients and mass removal rates were determined as functions of air pressure, which varied from 1 atm to 3.5 mtorr. The data from both coupling coefficients and mass removal rates show that there is a sharp transition region ranging between 1.0 and 10 torr. In this region, the momentum imparted to the target via air breakdown appears comparable to the momentum due to the breakdown on the target surface. At pressures exceeding 10 torr, the coupling to the target due to air breakdown dominates the ablation.

Nomenclature

A	=	oscillation amplitude
A_m	=	amplitude of free oscillations
B	=	damping coefficient in the oscillations amplitude equation
C_m	=	coupling coefficient
$C_{m,\mathrm{AB}}$	=	component of coupling coefficient due to air breakdown
$C_{m,\mathrm{abl}}$	=	ablative component of coupling coefficient
D	=	distance between ballistic pendulum and the ruler
d	=	displacement of the laser spot projected on the ruler
E	=	laser pulse energy
E_{air}	=	laser pulse energy consumed due to addition of air
g	=	acceleration due to gravity
I	=	moment of inertia of the pendulum
I_{sp}	=	specific impulse
k	=	spring constant
L	=	angular momentum
l	=	moment arm
l_c	=	distance from the pivot to the center of mass
M	=	mass of ablated propellant
m	=	mass of the pendulum
P	=	linear momentum
P_{AB}	=	component of linear momentum due to air breakdown
P_{abl}	=	component of linear momentum due to ablated mass of propellant
Q^*	=	specific ablation energy
t	=	time
v	=	mean velocity of ablated mass
α	=	friction term
ΔD	=	displacement of ballistic pendulum
θ	=	angular displacement of ballistic pendulum
θ_m	=	maximum angular displacement of ballistic pendulum in absence of damping
χ	=	efficiency
ω	=	angular velocity of a freely oscillating pendulum

Received 15 June 2004; revision received 26 May 2005; accepted for publication 18 July 2005.

*Associate Professor, Department of Physics. Member AIAA.
†Graduate Student, Department of Physics. Student Member AIAA.
‡Research Professor, Institute of Electronics.

Introduction

SYSTEMATIC studies on rocket propulsion using a laser as a remote energy source were started after the seminal work of Kantrowitz in 1972.[1] Since then, numerous investigations have been devoted to study the physics of laser propulsion (LP).[2–4] Setting aside the techniques employing direct light momentum transfers[5] (laser-driven light sails) and laser-induced vaporization of targets[6] or heat exchangers[7] (thermal laser propulsion), we are left with basically two main modes of operation for laser propulsion, both based on laser-induced breakdown. One of those modes is ablative LP (ALP), providing thrust from ablation on the surface of solid propellants in vacuum. Another one uses laser-induced breakdown of air or other gases near the light-focusing surface of the vehicle.[2] To distinguish the latter case from ALP, we will call the second mode gas breakdown LP (GBLP). Both modes show a strong dependence on the laser pulse duration and have quite different dynamics, propellant consumption regimes, and geometry.[8] The choice of LP mode should be determined from mission requirements and available lasers. When such choice is made, the entire design of the LP engine will be based on the chosen mode. (Some discussions on these matters may be found in Ref. 8.)

In a series of studies that were completed by the LP group at the University of Alabama in Huntsville,[9–14] ALP appeared to be a promising concept. However, the purely ALP mode, that is, regime when momentum transfer to the target is dominated by direct ablative mass removal, requires relatively short laser pulses (0.5 ns or less) to avoid plasma shielding.[9,12,13] The development of high-power lasers providing such pulsewidths is currently in progress, which hopefully will lead to implementation of the ALP technique in the near future.[15] In the meantime, it would be interesting to employ currently available high-power lasers to compare the performance under both ALP and GBLP modes. The comparison could be conducted along such propulsive parameters as specific impulse I_{sp}, coupling coefficient C_m, efficiency χ, etc. This work presents our first effort of this kind. We have attempted to address the distribution of propulsive energy between air and solid propellant, characterized through propulsion figures of merit assessed as functions of air pressure. As we expected, starting from 1 atm, the reduction of air pressure should lead to eventual transfer from GBLP based on breakdown in air in the presence of metal targets to a quasi-ablative regime. The prefix quasi used here indicates that, from the pulse duration aspect, the ablative regime under 200-ns-wide laser pulses

will be quite insignificant due to plasma shielding. Moreover, under our experimental conditions, that is, the mentioned pulse durations and the irradiance $\sim 10^{10}$ W/cm^2, the major momentum transfer must be associated with the development of laser-supported detonation (LSD) waves.[16] From this point of view, the notion of air vs propellant breakdown used as a line of division of the observed phenomena becomes quite blurred. In that sense, in the discussion of the data measured at different air pressures, the phrase air vs propellant breakdown can be translated as lower (or no) vacuum vs higher vacuum, which will set our line of comparison.

We believe that the air pressure effect on propulsive parameters is quite an interesting object of study, especially in a view of a surprising lack of such experimental data. Indeed, the studies conducted during the early years of LP demonstrated that air breakdown in atmosphere decouples the energy from the metal target.[17] As a consequence, the choice of a particular metal as a propellant under such regimes has little effect on the propulsive performance, although the presence of a metal is crucial for plasma ignition.[18] In other words, GBLP would dominate even with the laser pulses focused on metal surfaces, although the breakdown in evaporated metal and LSD dynamics would take a crucial part in these phenomena. At this point one may ask a question: Should we expect the cessation of GBLP regime if the air pressure is gradually reduced? Addressing this question by a simple experiment was the initial reason for starting the study. The preliminary results of our study were reported in Ref. 19, showing that the coupling coefficient in vacuum is comparable to that under air breakdown conditions. However, we were looking for an opportunity to address the partition of propulsive energy between air and solid breakdown vs air pressure, presuming, of course, that the notion of such partition would have any meaning in the first place. Further experiments were needed to deduce coupling coefficient as a function of air pressure. We chose solid aluminum as the target in the experiments in view of its extensive use in the past,[16] as well as in more resent LP studies.[11] In addition to coupling coefficients, we measured mass removal rates, which helped us to set a baseline for reckoning the ablative component in observed processes. By evaluating coupling coefficients and mass removal rates as functions of air pressure, we attempted to deduce the partition of propulsive energy between air and solid propellants.

Experimental Technique

The experimental setup is shown in Fig. 1. The laser system (Fig. 1, 1) comprises a transversely excited atmospheric (TEA) CO_2 laser (Lumonics, TEA-103) and laser control unit (Lumonics, 100 Control). The laser is set to output single pulse with energy 10.6 J and pulse width [full width at half maximum (FWHM)] $\sim$200 ns at wavelength 10.6 μm. The pulse energy was measured by an energy/power meter (Scientech, 365). Pulse profiles were measured by an ultrafast pyroelectric detector (Molectron, P5) connected to a digital oscilloscope (Tektronix TDS 460A). Figure 2 shows a photograph of the laser footprint near the output coupler. The footprint has a square shape of area 30×30 mm^2. The temporal profile of the laser pulse as seen on the oscilloscope is also given in Fig. 2. The FWHM of the front peak is 200 ns. The energy carried by the front peak was about 40% of the total pulse energy.

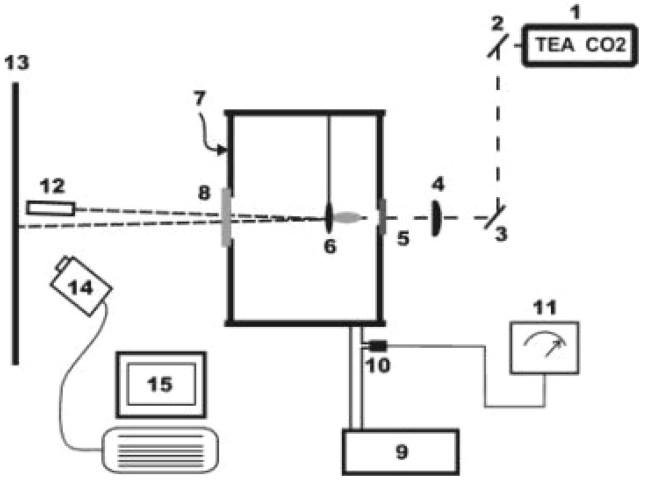

Fig. 1 Experimental setup.

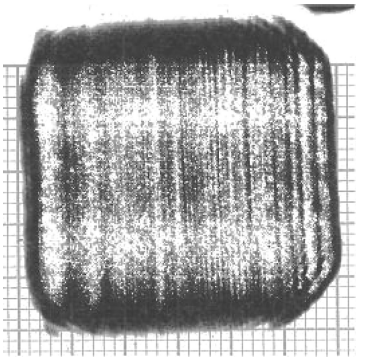

a)

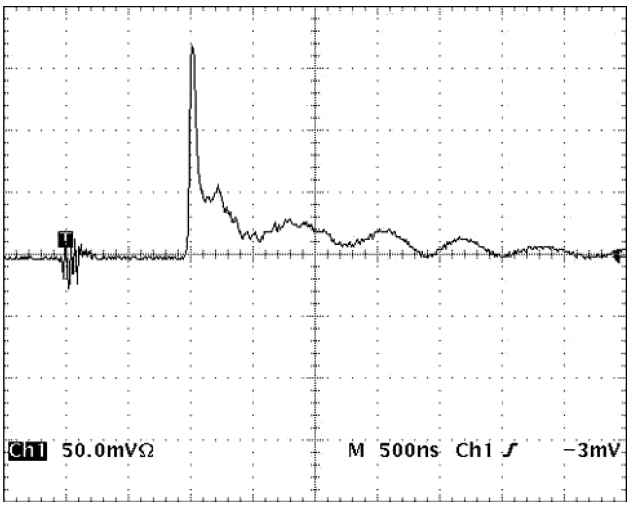

b)

Fig. 2 Output signatures of TEA CO_2 laser: a) laser pulse footprint and b) its temporal profile as seen on the oscilloscope.

The laser pulse was directed by a set of mirrors (Fig. 1, 2 and 3) toward a planoconvex ZnSe lens (Fig. 1, 4) which focused it through a ZnSe optical window (Fig. 1, 5) onto an aluminum sample. The window transmitted $\sim$74% of laser energy. The sample was mounted on a ballistic pendulum (Fig. 1, 6) placed in a vacuum chamber (Fig. 1, 7). The AR-coated lens (Fig. 1, 4), has focal length of 30.5 cm. The lens was mounted on an adjustable translation stage. The energy of the laser pulse delivered to the target is $\sim$6.8 J at the focal spot of area $\sim 1.7 \times 10^{-3}$ cm^2, corresponding to a fluence of $\sim 4 \times 10^3$ J/cm^2 and the peak irradiance of $\sim 10^{10}$ W/cm^2. The vacuum chamber has cylindrical shape of 22 in. diameter and 31 in. height with four windows. Aside from a ZnSe window (Fig. 1, 5), the other three windows (Fig. 1, 8) are made of glass. A roughing pump (Fig. 1, 9) (Pfeiffer Balzers, DUO 016 B) was used to provide the pressure down to 3.5 mtorr. The higher pressures were achieved by turning the pump off and letting air into the chamber through the ball valve. Starting from $\sim$1.0 torr, the chamber holds the preset pressures for hours, that is, much longer than required for the measurements. The air pressure in the chamber was measured by two thermocouple gauge sensors (Fig. 1, 10) (Thermistor Gauge Tube GT-034 for the pressure range 2 torr–1 atm and a Kurt Lesker KJL-6000 for the pressure range 3.5 mtorr–2.0 torr). The pressure measured by the thermocouple gauge sensor was read by controllers (Fig. 1, 11): CVC Products, Inc., GT-340A used for the pressure range 2 torr–1 atm and Kurt Lesker IG4400 for the pressure range 3.5 mtorr–2.0 torr.

The displacements of the ballistic pendulum were detected using a lightweight mirror attached to the back of the ballistic pendulum,

irradiated with an He–Ne laser (Fig. 1, 12) (Melles Griot, 05-LLR-811). The beam of the He–Ne laser was directed to the mirror through the glass window (Fig. 1, 8), and then the reflected spot was projected onto a wall ruler (Fig. 1, 13). Coupling coefficients were derived from the ballistic pendulum displacements, recorded by a digital video camcorder (Fig. 1, 14) (Sony DCR-TRV11). The movies were transferred to a personal computer (Fig. 1, 15) via video editing software (Ulead VideoStudio™ 5.0) that provides avi files of 29.9 frames per second. Video converting software (1st Video Converter 5.2.4) and Adobe Photoshop 7.0 were used to convert the avi files to sequences of frames for each experiment, and these frames were analyzed using a set of programs written in Mathematica (version 4.0). The mass removal per laser pulse was measured by a precision balance (Mettler AE 163).

Results and Discussion

Coupling Coefficients

To determine the magnitude of the impulse imparted to the target, we used a ballistic pendulum. Energy is imparted to the aluminum target attached to the pendulum. A probe laser is reflected off of the opposite face of the pendulum and is seen on a ruled surface at 6.66 m away from the pendulum. The motion of the pendulum is restricted to the vertical plane with simple geometry presented in Fig. 3.

The distance between the ballistic pendulum at rest and the ruler is D, whereas d is the displacement of the laser spot at the ruler, and θ is the angular displacement of the pendulum. When small linear and angular displacements of the pendulum, are assumed, that is, $D \gg \Delta D$, $\sin\theta \approx \theta$, the angular displacement of the pendulum and linear displacement of laser spot d are related as

$$\theta = d/2D \tag{1}$$

A typical time-displacement diagram of the probing laser spot is shown in Fig. 4. Figure 4 shows the observed oscillations of the ballistic pendulum. As one can see, the amplitude of the pendulum displacement is linearly decreasing with time, and not exponentially, as one should expect for the motion of a damped oscillator.[20] This

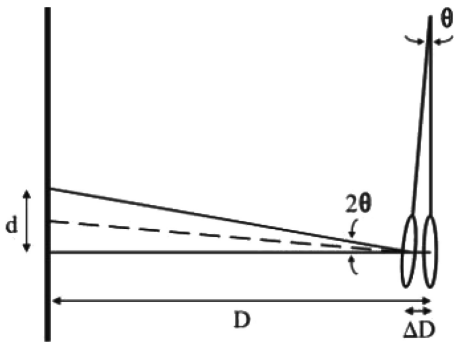

Fig. 3 Geometry of pendulum displacement: ----, normal to pendulum surface at the angular displacement θ.

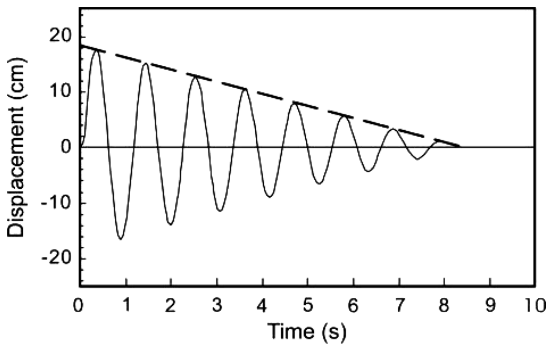

Fig. 4 Oscillation of ballistic pendulum in air at atmospheric pressure: straight line is the linear fit to the amplitude.

type of oscillation, known as Coulomb friction, is described by the equation of motion[21]

$$I\ddot{\theta} + \alpha\,\mathrm{sign}(\dot{\theta}) + k\theta = 0 \tag{2}$$

where I is the moment of inertia of the pendulum, $\mathrm{sign}(\dot{\theta})$ is the direction of the oscillation, whereas the friction term α is a constant, representing both air resistance and friction at the pivot. Parameter k is the spring constant, so that $\sqrt{(k/I)}$ is the frequency of the free oscillation. A linear fit to the oscillation envelope, shown as the straight line in Fig. 3, can be written as

$$A = A_m + Bt \tag{3}$$

where A_m refers to the amplitude of the nondamped case.[21] The amplitude of the free oscillation A_m, deduced from Eq. (3) at $t = 0$, was used for the derivation of coupling coefficients. The coupling coefficient C_m is defined as a ratio of the momentum P imparted to the target to the laser pulse energy E,

$$C_m \equiv P/E \tag{4}$$

The linear momentum P is related to the angular momentum L assuming that the moment arm is normal to the direction of the linear momentum as

$$P = L/l = I\omega/l \tag{5}$$

where l is the magnitude of the moment arm, that is, the distance between the pivot point of the pendulum and the focal point (the point where the thrust is imparted), and ω can be defined as an angular velocity of a freely oscillating pendulum. Then, from energy conservation,

$$\tfrac{1}{2}I\omega^2 = mgl_c(1 - \cos\theta_m) \tag{6}$$

where g is the gravitational acceleration, l_c is the length of the pendulum, and θ_m is the angular displacement corresponding to A_m.

From Eqs. (1) and (3–6) we can express the coupling coefficient as

$$C_m = (1/El)\sqrt{2mgIl_c}\sqrt{1 - \cos(A_m/2D)} \tag{7}$$

Therefore, from the determined free-oscillation amplitude A_m and for known pulse energy, pendulum mass, and all distances, we can determine the coupling coefficient.

Coupling coefficients deduced from the experiment using Eq. (7) are shown as function of air pressure in Fig. 5. Each data point represents the mean value of five separate measurements, and the error bar shows one standard deviation. As one can see from Fig. 5, the coupling coefficient shows different behavior for lower pressures (approximately 1 torr and below), compared to higher pressures (above 10 torr). At the low pressures (higher vacuum), corresponding to the 3.5–300 mtorr pressure range, the coupling coefficient appears pressure independent. As air pressure increases, the coupling coefficient increases steadily until the upper limit on pressure is reached (1 atm). A transition region dividing two observed regimes appears between 1.0 and 10 torr. In this region, the curve in Fig. 5 has a shoulder, the nature of which will be explained subsequently.

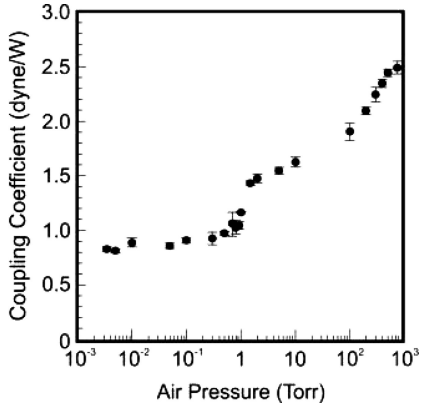

Fig. 5 Coupling coefficient vs air pressure.

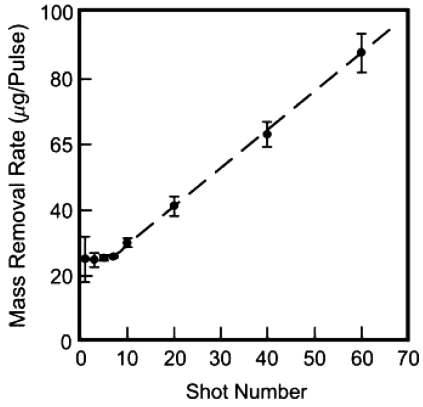

Fig. 6 Mass-removal rate vs laser shot number (measured at 5-mtorr pressure): - - - -, data trend.

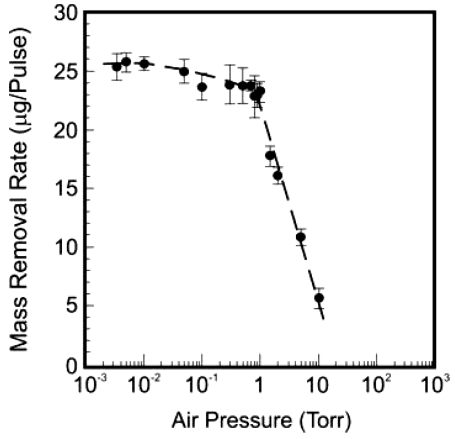

Fig. 7 Mass-removal rate vs air pressure: - - - -, data trend.

Mass Removal Rates

Mass removal rate can be used as a measure of the ablative component in the overall momentum imparted by the laser pulse/target surface interaction. Of course, that would require certain conditions to be met. One has to assume that, within the given range of experimental conditions, effects of redeposition can be ignored and one mass-removal mechanism such as, for example, normal (surface) vaporization is not mixed with another, such as, for example, volume vaporization (or phase explosions).[22] Apparently, in a wide range of experimental conditions, such as air pressures in this work, one has to be very cautious about applying such assumptions. Nevertheless, we used mass-removal rate as an indicator of ablative processes, and it appears quite helpful for our assessments.

Figure 6 shows the measured mass-removal rates vs the number of laser shots. (The time between shots was maintained for at least 1 min.) Similar data were observed for pressures in the range of 3.5–50 mtorr. Each data point represents the mean of two measurements, and the error bar stands for one standard deviation. The data from the first five shots provided the most reproducible values.

After approximately five shots, mass-removal rate was gradually increasing with the shot number. The latter effect is presumably related to the removal of macroscopic particulates, which were visually observed. It is unclear why particulate removal was onset after the first five shots. Note that whereas the mass removal, as shown in Fig. 6, was increasing with larger than 5 shot numbers the value of coupling coefficient did not change. This observation indirectly supports our assumption on role of particulate removal: As we have reported earlier in Ref. 22, removal of such particulates has an adverse effect on momentum transfer due to relatively low (~100 m/s) ejection velocities. To avoid the complications due to dependence presented in Fig. 6, we choose to use an average over the first five shots for our mass-removal rate measurements.

Mass-removal rate as a function of air pressure is shown in Fig. 7. Each data point represents the mean value of five independent experiments, with the data averaged over the first five shots per experiment, whereas the error bar stands for one standard deviation. Mass-removal rate appears slowly decreasing with increasing pressure up to 1 torr, after that it drops sharply and reaches our measurement limit (1.0 μg) at 10 torr. When compared to Fig. 5, the data of Fig. 7 show obvious reciprocity between coupling coefficients and mass-removal rates. Moreover, the sharp change appears in both coupling coefficients and mass-removal rates for the same air pressure region 1.0–10.0 torr.

Discussion

Thus, as discussed in the preceding section, the presented experimental data on coupling coefficient and mass-removal rate as functions of air pressure show an interesting correlation. Both dependencies exhibit reciprocal behavior for pressures below 1 torr and above 10 torr, with a common transition region at pressures of 1.0–10.0 torr. Therefore, we assume that these two clearly distinct pressure regions present two concurrent processes, which we will call air breakdown in presence of metal targets at higher pressures and target breakdown, leading to target ablation at lower pressures, respectively. Because both processes are initiated under the same laser irradiation, it would be interesting to deduce the energy partition between them. To estimate such a partition, we assume that specific ablation energy Q^*, defined as an energy needed to ablate a unit mass of solid propellant, is a constant. In other words, Q^* is independent from air pressure. Now let us examine Fig. 7. At the lowest pressure, mass-removal rate stays constant at the level of ~25 μg/pulse. This would correspond to $Q^* = 2.7 \times 10^5$ J/g. Then conservation of energy can be presented as

$$E = E_{\text{air}} + Q^* M \tag{8}$$

where E is laser pulse energy at the target and M is the mass of removed propellant. E_{air} corresponds to the overall amount of energy consumed by air breakdown and all energy consuming processes caused by addition of air to the system, such as, for example, reflection of light by air plasma. Q^*M, aside from the energy consumed by the breakdown on the target, includes all energy-consuming processes that occurred in a vacuum. Those are, for example, a reflection from the sample surface and heat dissipated in the bulk of the sample. Then, using Eq. (8), we can calculate E_{air}. The results of such calculation are shown in Fig. 8. Each point of the curve represents the mean calculated out of five measured values, and the error bar stands for one standard deviation. As one can see from Fig. 8, the equal energy partition, that is, intersection of Q^*M and E_{air} curves, occurs at ~3.5 torr. The intersection lies precisely within experimentally observed transition region. The phenomena driven at higher air pressures, which we denote as air breakdown in the presence of metal targets, becomes dominant at pressures exceeding ~10 torr.

A similar approach can be used for estimation of linear momentum $\boldsymbol{P}$ imparted to the solid target by the laser pulse. Again, we

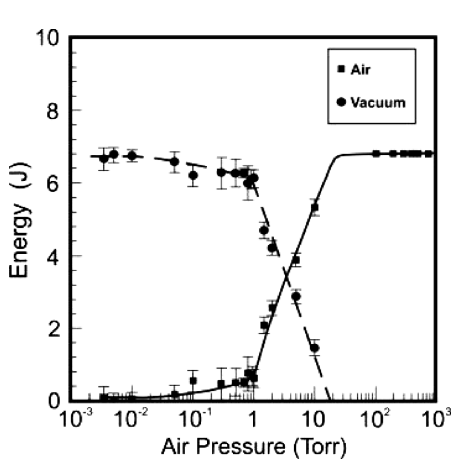

Fig. 8 Energy partition vs air pressure; data trends: ——, air and - - - -, vacuum.

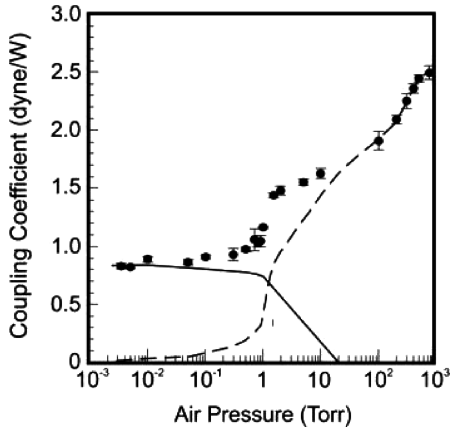

Fig. 9 Coupling coefficient vs air pressure: ——, ablative and - - - -, air-breakdown components of coupling coefficient.

assume that there are two main components of this momentum: $\boldsymbol{P}_{\text{abl}}$, which originates from the jet of ablated solid material, and $\boldsymbol{P}_{\text{AB}}$ imparted at higher pressures, when air breakdown dominates,

$$\boldsymbol{P} = \boldsymbol{P}_{\text{abl}} + \boldsymbol{P}_{\text{AB}} = M\boldsymbol{v} + \boldsymbol{P}_{\text{AB}} \tag{9}$$

Assuming that 1) $\boldsymbol{P}_{\text{AB}}$ at air pressure of 3.5 mtorr can be neglected and 2) the mean velocity of material jet $\boldsymbol{v}$ is a constant over the whole range of air pressures, we can deduce $\boldsymbol{P}_{\text{AB}}$. Dividing both parts of Eq. (9) by laser pulse energy E will convert the equation into terms of coupling coefficients as

$$C_m = C_{m,\text{abl}} + C_{m,\text{AB}} \tag{10}$$

where $C_{m,\text{abl}}$ and $C_{m,\text{AB}}$ are components of the coupling coefficient, presenting ablative and higher pressure (air-breakdown) processes, respectively.

Figure 9 shows our estimation, where the overall coupling coefficient is presented as a function of pressure (Fig. 5) shown as a sum of two components: ablative and air breakdown (pressure dependent). The point of equal partition of the $C_{m,\text{abl}}$ and $C_{m,\text{AB}}$ is observed at ~1.2 torr, that is, within the same transition region, as the earlier presented energy partition. The already noted shoulder in the dependence of experimentally determined coupling coefficient appears above the transition region, where both components have comparative values. This shoulder ends at pressures above 10 torr, when the contribution from ablation becomes negligible.

Thus, we can conclude that using simple assumptions, such as $Q^* = \text{const}$, we have been able to extract the ablative component from the coupling coefficient curve measured for a range of pressures varied over five orders of magnitude. The transition region was independently observed on coupling coefficient and mass-removal rate dependencies. The coupling coefficient in the vacuum, that is, the coupling due to ablation, appeared as approximately one-third of the coupling coefficient observed at atmospheric pressure.

In these experiments we did not have an opportunity to measure exhaust velocity in the range of used air pressures, we just estimated it for vacuum limit. Note that the obtained value, $v = 2.2 \pm 0.1$ km/s, appeared about the same as an actual experimentally measured exit velocities (2 km/s) reported for Myrabo Laser Lightcraft (MLL) augmented with Delrin propellant.[23] Thus, we have a reason to believe that the data reported in this paper are close to realistic, lightcraft conditions. Of course, in the referenced MLL study, the tests were conducted at atmospheric pressures.

Also, there is a question of at what altitude atmospheric pressure is 10 torr, that is, at what altitude would even hovering MLL not be able to support itself in airbreathing mode. According to Ref. 24, this altitude is 30 km. Of course, moving MLL will experience the lack of oxygen at even lower altitudes. Thus, the ablative regime will be required in the early stage of the vehicle ascent.

Table 1 presents the coupling coefficient, the specific impulse, and the internal efficiency χ observed on aluminum targets in ALP regime[12] and in this work at a pressure of 3.5 mtorr. The efficiency was calculated as $\chi = 0.5 C_m v$. (For details on calculation of ALP efficiency χ, see Ref. 12.) Thus, as one can see from Table 1, the coupling coefficient of the ablative component with the TEA CO_2 laser appears of the same order with ALP, whereas the specific impulse and, consequently, the efficiency are about 20 times less. At this point we can only assume that the specific impulse deduced from our experiments is relatively low because of inefficient utilization of propellant mass. Some low-velocity removal of particulates might be a reason for these data. However, this question deserves further studies. We must admit that the data presented in this paper are deduced from experiments limited by means and by certain assumptions. Therefore, any generalization at this point would be rather presumptuous. Still, even on the basis of these data, a clear advantage of ALP compared to a longer pulsed TEA CO_2 system can be seen.

Table 1 Propulsive characteristics of aluminum at air pressure 3.5 mtorr

Source	I_{sp}, s	C_m, dyne/W	χ, %
ALP, Ref. 12	4200	0.9	18
This work	226 ± 8	0.83 ± 0.02	0.9 ± 0.04

Conclusions

Coupling coefficients and mass removal rates for aluminum targets irradiated by a pulsed TEA CO_2 laser have been determined as functions of air pressure in the range from 3.5 mtorr to 1 atm. The main results are as follows:

1) The functions show reciprocal correlation and are characterized by the same transition region from 1 to 10 torr. The transition region presents the pressures when ablative momentum-transfer mechanism, dominating at higher vacuum, coexists with air breakdown momentum transfers, characteristic for higher pressures.

2) Equal partition of energy and linear momentum between these two modes is observed at pressures of 3.5 and 1.2 torr, respectively. The ablative component of the coupling coefficient reached 0.83 ± 0.02 dyne/W, which is one-third of the maximum value of C_m observed at atmospheric pressure.

3) The comparison of propulsive characteristics achieved with TEA CO_2 laser with ALP regime show that, although coupling coefficients are practically the same, specific impulse and efficiency are about 20 times higher for ALP conditions.

Acknowledgment

The authors acknowledge all discussions and technical help provided by former and current members of the Laser Propulsion Group at the University of Alabama in Huntsville.

References

[1]Kantrowitz, A., "Propulsion to Orbit by Ground Based Lasers," *Aeronautics and Astronautics*, Vol. 9, No. 3, 1972, pp. 40–42.

[2]Pirri, A. N., Monsler, M. J., and Nebolsine, P. E., "Propulsion by Absorption of Laser Radiation," *AIAA Journal*, Vol. 12, No. 9, 1974, pp. 1254–1261.

[3]Phipps, C. R., Turner, T. P., and Harrison, R. F., "Impulse Coupling to Target in Vacuum by KrF, HF, and CO_2 Single Pulse Laser," *Journal of Applied Physics*, Vol. 64, No. 3, 1988, pp. 1083–1096.

[4]Schall, W. O., Eckel, H.-A., Mayerhofer, W., Riede, W., and Zeyfang, E., "Comparative Lightcraft Impulse Measurements," *High-Power Laser Ablation IV, Proceedings of SPIE*, edited by C. R. Phipps, Vol. 4760, Society of Photo-Optical Instrumentation Engineers (International Society for Optical Engineering), Bellingham, WA, 2002, pp. 908–917.

[5]Marx, G., "Interstellar Vehicle Propelled by Terrestrial Laser Beam," *Nature*, Vol. 211, No. 5044, 1966, pp. 22, 23.

[6]Bunkin, F. V., and Prokhorov, A. M., "Using Laser Energy Source for Generation of Reactive Thrust," *Soviet Physics—Uspekhi*, Vol. 119, No. 3, 1976, pp. 425–446 (in Russian).

[7]Jordin Kare, T., "Near-Term Laser Launch Capability: The Heat Exchanger Thruster," *First International Symposium on Beamed Energy Propulsion, Huntsville, Alabama, 2002, American Institute of Physics Conference Proceedings*, edited by A.V. Pakhomov, Vol. 664, American Inst. of Physics, Melville, NY, 2003, pp. 442–453.

[8]Rezunkov, Y., and Pakhomov, A. V., "Perspective In-Space Laser Propulsion Demonstrator Mission," *Second International Symposium on Beamed Energy Propulsion, Sendai, Japan, October 20–23, 2003, American Institute of Physics Conference Proceedings*, edited by K. Komurasaki, Vol. 702, American Inst. of Physics, Melville, NY, 2004, pp. 442–453.

[9]Pakhomov, A. V., Thompson, M. S., and Gregory, D. A., "Specific Impulse and Other Characteristics of Elementary Propellants for Ablative Laser Propulsion," *AIAA Journal*, Vol. 40, No. 5, 2002, pp. 947–952.

[10]Pakhomov, A. V., Thompson, M. S., Swift, W., Jr., and Gregory, D. A., "Ablative Laser Propulsion: Specific Impulse and Thrust Derived from Force Measurements," *AIAA Journal*, Vol. 40, No. 11, 2002, pp. 2305–2311.

[11]Pakhomov, A. V., Thompson, M. S., and Gregory, D. A., "Ablative Laser Propulsion: A Study of Specific Impulse, Thrust and Efficiency," *First International Symposium on Beamed Energy Propulsion, Huntsville, Alabama, 2002, American Institute of Physics Conference Proceedings*, edited by A. V. Pakhomov, Vol. 664, American Inst. of Physics, Melville, NY, 2003, pp. 194–205.

[12]Thompson, M. S., Herren, K. A., Lin, J., and Pakhomov, A. V., "Effects of Time Separation on Double-Pulsed Laser Ablation of Graphite," *First International Symposium on Beamed Energy Propulsion, Huntsville, Alabama, 2002, American Institute of Physics Conference Proceedings*, edited by A. V. Pakhomov, Vol. 664, American Inst. of Physics, Melville, NY, 2003, pp. 206–213.

[13]Pakhomov, A. V., Cohen, T., Lin, J., Thompson, M. S., and Herren, K., "Ablative Laser Propulsion: An Update, Part I," *Second International Symposium on Beamed Energy Propulsion, Sendai, Japan, October 20–23, 2003, American Institute of Physics Conference Proceedings*, edited by K. Komurasaki, Vol. 702, American Inst. of Physics, Melville, NY, 2004, pp. 166–177.

[14]Pakhomov, A. V., Lin, J., and Thompson, M. S., "Ablative Laser Propulsion: An Update, Part II," *Second International Symposium on Beamed Energy Propulsion, Sendai, Japan, October 20–23, 2003, American Institute of Physics Conference Proceedings*, edited by K. Komurasaki, Vol. 702, American Inst. of Physics, Melville, NY, 2004, pp. 178–189.

[15]Pakhomov, A. V., and Gregory, D. A., "Ablative Laser Propulsion: An Old Concept Revisited," *AIAA Journal*, Vol. 38, No. 4, 2000, pp. 725–727.

[16]Pirri, A. N., Root, R. G., and Wu, P. K. S., "Plasma Energy Transfer to Metal Surfaces Irradiated by Pulsed Lasers," *AIAA Journal*, Vol. 16, No. 12, 1978, pp. 1296–1304.

[17]Pirri, A. N., Schlier, R., and Northam, D., "Momentum Transfer and Plasma Formation Above a Surface with a High-Power CO_2 Laser," *Applied Physics Letters*, Vol. 21, No. 1, 1972, pp. 79–81.

[18]Weil, G., Pirri, A., and Root, R., "Laser Ignition of Plasma Off Aluminum Surfaces," *AIAA Journal*, Vol. 19, No. 4, 1981, pp. 460–469.

[19]Tan, R., Lin, J., Hughes, J., and Pakhomov, A. V., "Experimental Study of Coupling Coefficients for Propulsion on TEA CO_2 Laser," *Second International Symposium on Beamed Energy Propulsion, Sendai, Japan, October 20–23, 2003, American Institute of Physics Conference Proceedings*, edited by K. Komurasaki, Vol. 702, American Inst. of Physics, Melville, NY, 2004, pp. 122–128.

[20]Landau, L. D., and Lifshitz, E. M., *Mechanics*, Vol. 1 of Course of Theoretical Physics, 3rd ed. Pergamon Press, Oxford, 1976, pp. 74–77.

[21]Peters, R., and Pritchett, T., "The Not-So-Simple Harmonic Oscillator," *American Journal of Physics*, Vol. 65, No. 11, 1997, pp. 1067–1073.

[22]Pakhomov, A. V., Thompson, M. S., and Gregory, D. A., "Laser-Induced Phase Explosions in Lead, Tin and Other Elements: Microsecond Regime and UV-Emission," *Journal of Physics D: Applied Physics*, Vol. 36, Aug. 2003, pp. 2067–2075.

[23]Larson, C. W., and Mead, F. B., Jr., "Energy Conversion in Laser Propulsion," AIAA Paper 2001-0646, Jan. 2001.

[24]*CRC Handbook of Chemistry and Physics*, 56th ed., edited by R. C. Weast, CRC Press, Cleveland, OH, 1975, p. F-204.

R. Lucht
Associate Editor